iScience

CellPress
OPEN ACCESS

Article

3D blood-brain barrier-organoids as a model for Lyme neuroborreliosis highlighting genospecies dependent organotropism

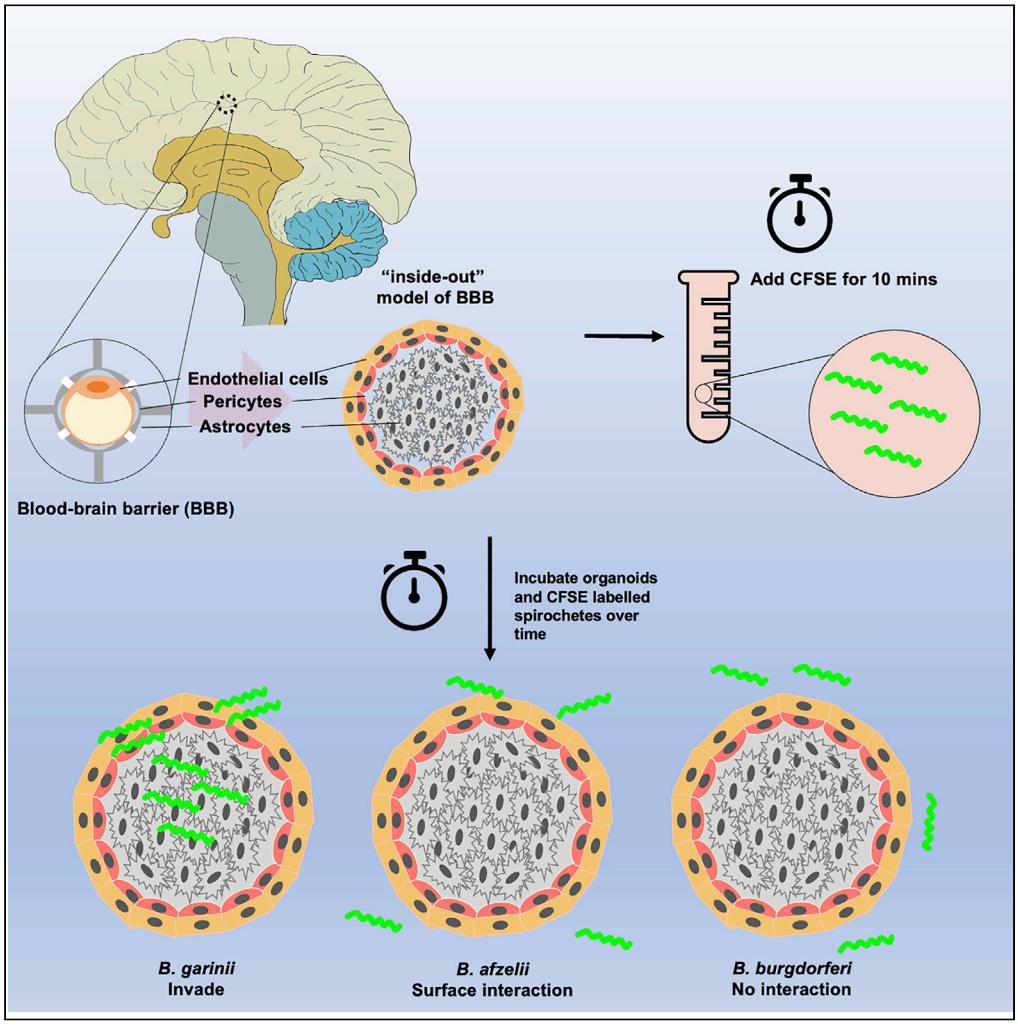

Yvonne Adams, Anne Skovsbo Clausen, Peter Østrup Jensen, ..., Andreas Kjaer, Anne-Mette Lebech, Anja R. Jensen

yadams@sund.ku.dk (Y.A.)
atrj@sund.ku.dk (A.R.J.)

Highlights

Human derived blood-brain barrier organoids support *Borrelia* spp. invasion

Borrelia garinii preferentially invades organoids

Borrelia spp. exposure triggers a loss of tight junctions

Organoid structural integrity is significantly reduced after *Borrelia* spp. exposure

Adams et al., iScience 26, 105838
January 20, 2023 © 2022
https://doi.org/10.1016/j.isci.2022.105838

iScience

CellPress
OPEN ACCESS

Article

3D blood-brain barrier-organoids as a model for Lyme neuroborreliosis highlighting genospecies dependent organotropism

Yvonne Adams,[1,12,*] Anne Skovsbo Clausen,[2] Peter Østrup Jensen,[3,8,9] Malin Lager,[4] Peter Wilhelmsson,[4,5] Anna J. Henningson,[4,5] Per-Eric Lindgren,[4,5] Daniel Faurholt-Jepsen,[6] Helene Mens,[6] Peter Kraiczy,[7] Kasper Nørskov Kragh,[8,9] Thomas Bjarnsholt,[8,9] Andreas Kjaer,[2] Anne-Mette Lebech,[6,10,11] and Anja R. Jensen[1,11,*]

SUMMARY

Lyme neuroborreliosis (LNB), a tick-borne infection caused by spirochetes within the *Borrelia burgdorferi* sensu lato (s.L.) complex, is among the most prevalent bacterial central nervous system (CNS) infections in Europe and the US. Here we have screened a panel of low-passage *B. burgdorferi* s.l. isolates using a novel, human-derived 3D blood-brain barrier (BBB)-organoid model. We show that human-derived BBB-organoids support the entry of *Borrelia* spirochetes, leading to swelling of the organoids and a loss of their structural integrity. The use of the BBB-organoid model highlights the organotropism between *B. burgdorferi* s.l. genospecies and their ability to cross the BBB contributing to CNS infection.

INTRODUCTION

Lyme borreliosis (LB), the most prevalent vector-borne infection in Europe and the US, is an emerging tick-borne infection caused by spirochetes belonging to the *Borrelia burgdorferi* sensu lato (s.L.) complex. More than 20 different *B. burgdorferi* s.l. genospecies have been identified. Not all *B. burgdorferi* s.l. genospecies are known to be pathogenic to humans, whereas in the US *B. burgdorferi* sensu stricto (s.s.) is the predominant genospecies associated with LB. In Europe, *Borrelia garinii* and *Borrelia afzelii* are the most common genospecies in humans.[1]

The clinical manifestations of LB are diverse, with the expanding skin lesion, erythema migrans being the most common manifestation of LB. Dissemination of *B. burgdorferi* s.l. to the central nervous system (CNS) causing Lyme neuroborreliosis (LNB) has been reported to occur in approximately 10–15% of all cases of LB.[1,2]

Many aspects of the pathogenesis of LNB are still largely unknown, specifically how *B. burgdorferi* s.l. gains access to the CNS. Generally, dissemination to the CNS in humans is considered to occur through the bloodstream or along peripheral nerves.[3,4] In Europe, early LNB in adults mainly manifests as a subacute painful meningoradiculitis and/or cranial nerve palsy and is typically associated with infection with *B. garinii*, which is particularly neurotropic.[5,6] In contrast, the most frequent manifestation of LNB among patients in the US is lymphocytic meningitis caused by *B. burgdorferi* s.s. Thus, it is possible that the mechanism of dissemination to the nervous system is different in Europe and the US and depends on individual genospecies of *B. burgdorferi* s.l. and their ability to cross the blood-brain barrier (BBB).

The mechanism of how the spirochetes pass the BBB is not known although both paracellular and transcellular penetration, in addition to the spirochete-induced expression of plasminogen and metalloproteinases activators influencing the connections (tight-junctions) in the BBB have been proposed.[3,4] However, further investigations to understand the pathogenesis of LNB are required but are limited by the lack of adequate animal models. Multiple animal types ranging from dogs, rhesus monkeys, New Zealand white rabbits, guinea pigs, and various strains of inbred mice have been used to model *B. burgdorferi* infection[7–10]; however, no single animal model fully recapitulates the disease progression observed in humans, and variation in responses between animal models is also observed.[7] Recent studies using the C3H strain of inbred mice have demonstrated colonization of the dura mater during acute and late disseminated infection, however in human LNB, spirochetes have been observed perivascular, and within the

[1]Centre for Medical Parasitology, Department of Immunology and Microbiology, Faculty of Health and Medical Sciences, University of Copenhagen, Maersk Tower, Blegdamsvej 3B, 2200 Copenhagen N, Denmark

[2]Department of Clinical Physiology and Nuclear Medicine & Cluster for Molecular Imaging, Copenhagen University Hospital-Rigshospitalet, Copenhagen, Denmark

[3]Department of Biomedical Sciences, University of Copenhagen, University Hospital-Rigshospitalet, Copenhagen, Denmark

[4]National Reference Laboratory for Borrelia and Other Tick-Borne Bacteria, Division of Clinical Microbiology, Laboratory Medicine, Region Jönköping County and Department of Biomedical and Clinical Sciences, Linköping University, Linköping, Sweden

[5]Division of Inflammation and Infection, Department of Biomedical and Clinical Sciences, Linköping University, Linköping, Sweden

[6]Department of Infectious Diseases, Copenhagen University Hospital-Rigshospitalet, Copenhagen, Denmark

[7]Institute of Medical Microbiology and Infection Control, University Hospital of Frankfurt, Goethe University Frankfurt, Frankfurt, Germany

[8]Department of Clinical Microbiology, Copenhagen University Hospital-

Continued

Table 1. *Borrelia burgdorferi* sensu lato (complex) isolates used to generate experimental data

Isolate	Genospecies	Geographic origin	Isolate origin	Clinical diagnosis	Passage no.	References
ML23[a]	*B.burgdorferi sensu stricto*	USA	Tick	NA	NA	Ornstein et al.[11]
HB19	*B.burgdorferi sensu stricto*	USA	Blood	NA	NA	Ornstein et al.[11]
LU58	*B. afzelii*	Sweden	Skin	EM[b]	6	Ornstein et al.[11]
LU68	*B. afzelii*	Sweden	Skin	EM[b]	6	Ornstein et al.[11]
LU81	*B. afzelii*	Sweden	Skin	EM[b]	7	Ornstein et al.[11]
LU171	*B. afzelii*	Sweden	Skin	EM[b]	5	Ornstein et al.[11]
LU207	*B. afzelii*	Sweden	Skin	EM[b]	6	Ornstein et al.[11]
LU116	*B. garinii*	Sweden	Skin	EM[b]	6	Ornstein et al.[11]
LU118	*B. garinii*	Sweden	Skin	EM[b]	NA	Ornstein et al.[11]
LU190	*B. garinii*	Sweden	CSF	LNB[c]	NA	Ornstein et al.[11]
LU190 luc[d]	*B. garinii*	Sweden	CSF	NA	NA	Steere et al.[12]
LU222	*B. garinii*	Sweden	CSF	LNB[c]	NA	Steere et al.[12]

EM, erythema migrans; CSF, cerebrospinal fluid; LNB, Lyme neuroborreliosis; NA, not available.
[a]*B. burgdorferi* sensu stricto/ML23 pBBE22luc gene transfected.[13]
[b]Individuals diagnosed with EM were19–69 years of age.
[c]Individuals diagnosed with LNB were 4–7 years of age.
[d]*B. garinii* G1/pBBE22luc ectopically producing luciferase.

parenchyma.[14–19] To enter the brain, pathogens must first navigate the BBB; access can occur via direct transmigration such as that observed with *Neisseria meningitidis*,[20,21] *Plasmodium falciparum*,[22] or for example, *Listeria monocytogenes* that can either gain direct entry, or are transported indirectly via a trojan horse mechanism and carried across the BBB within infected leukocytes (reviewed in[23]). Growing evidence demonstrates the critical role of the BBB in neurodegenerative and neuropsychiatric diseases. Multiple neurodegenerative diseases such as Parkinson's and Alzheimer's disease have "leaky" barriers,[24,25] whereas depressive disorders have also been shown to have altered permeability.[26–28] Increasing our knowledge on how the spirochetal infection leads to the observed neural dysfunction, especially how *B. burgdorferi* s.l. crosses and impacts the BBB will be of paramount interest to not only understand the mechanisms driving the development of LNB, but for the development of preventative and adjunctive treatments. In addition, the ability of different clinical *B. burgdorferi* s.l. isolates to cross the BBB is unclear. To test this, we used a newly developed *in vitro* 3D BBB model and *B. burgdorferi* s.l. strains isolated from human patients.

RESULTS

Blood-brain barrier-organoids support invasion by *B. burgdorferi* sensu lato spirochetes

To model LNB and investigate the effect of *B. burgdorferi* s.l. on the BBB, a 3D organoid model was employed. The organoids comprise brain endothelial cells, pericytes, and astrocytes with a distinct cellular orientation comparable to that of the *in vivo* BBB (Figure S1).[29,30] To assess the impact of *Borrelia* on the BBB we used a panel containing eleven *B. burgdorferi* s.l. isolates isolated from clinical samples (skin biopsies or cerebrospinal fluid), and one a single *B. burgdorferi* s.s. isolate originated from an infected tick (Table 1). The isolates included five *B. garinii* (LNB associated), five *B. afzelii* (LB associated; erythema migrans), and two *B. burgdorferi* s.s. (LB associated; erythema migrans, or from a tick). The *Borrelia* spirochetes were maintained in culture under microaerobic conditions for seven days before staining with carboxyfluorescein succinimidyl ester (CFSE), because there are varying timepoints reported in the literature, co-incubation with the BBB-organoids was performed for 1, 4 and 24 h. CFSE was chosen to ensure no dye transfer from the spirochetes, unlike that observed with other dyes.[31] Organoids were also mock treated with spirochete media, to ensure any observed changes where due to the borreliae, and not the change in media composition. At the earliest time point (1 h), only a few spirochetes were observed interacting with the organoids (Figure 1A); however, by 4 h, multiple individual spirochetes were observed interacting with the organoid surface for a single *B. garinii* isolate (LU116). With this isolate, spirochetes were observed perpendicular to the surface of the organoid (Figure 1B left panel inset). In contrast, the 24-h timepoint showed multiple *B. garinii* isolates (LU116, 118, 190, 190 luc, and 222) having many bacterial aggregates of varying sizes colonizing not only to the surface of the BBB-organoids, but also extending to depths of

Rigshospitalet, Copenhagen, Denmark

[9]Costerton Biofilm Center, Department of Immunology and Microbiology, Faculty of Health and Medical Sciences, University of Copenhagen, Copenhagen, Denmark

[10]Department of Clinical Medicine, University of Copenhagen, Copenhagen, Denmark

[11]These authors contributed equally

[12]Lead contact

*Correspondence: yadams@sund.ku.dk (Y.A.), atrj@sund.ku.dk (A.R.J.)

https://doi.org/10.1016/j.isci.2022.105838

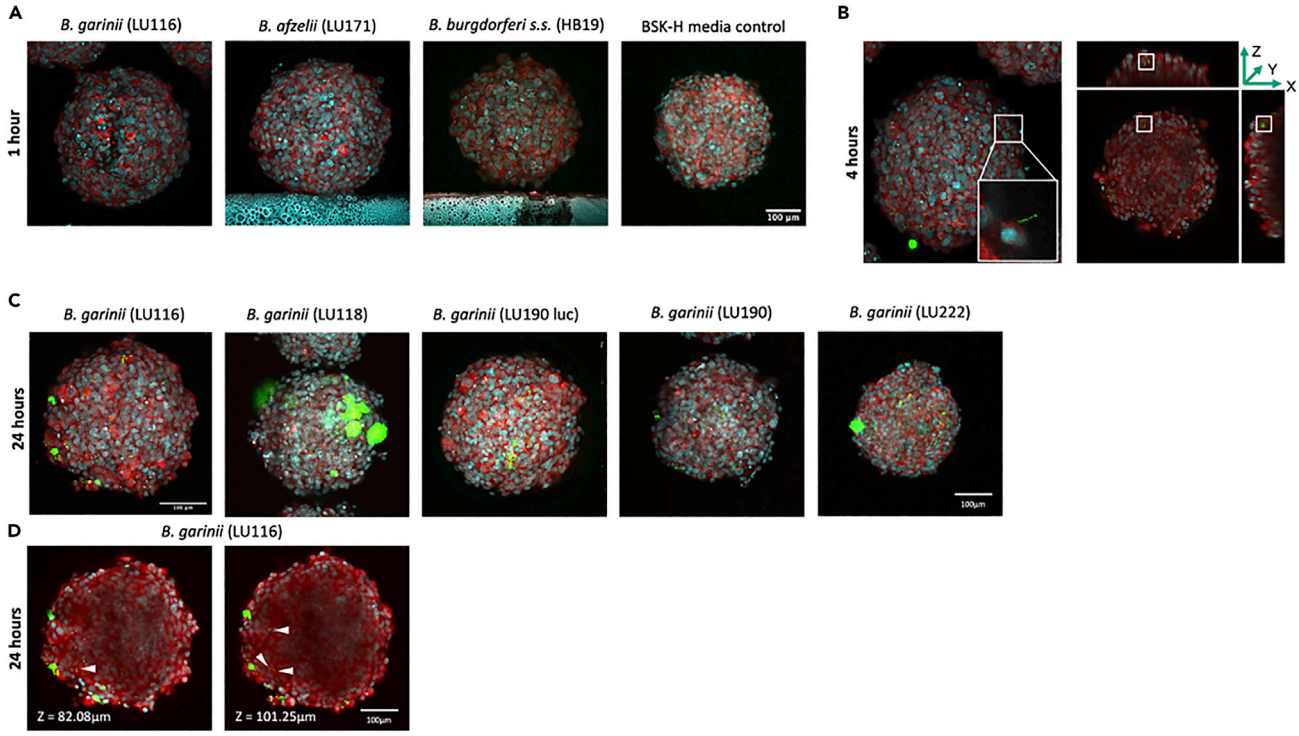

Figure 1. Blood-brain barrier organoids support entry of *Borrelia burgdorferi*

(A) 3D Z-projections of blood-brain barrier (BBB)-organoids (Magnification ×20) stained for *Borrelia burgdorferi* s.l. (CFSE, green), nuclei (DAPI, blue) and actin cytoskeleton (phalloidin, red). Scale bar 100 µm.

(B left panel) Z-projection of BBB-organoid exposed to *B. garinii* LU116 for 4 h. White box and inset shows higher magnification image of single spirochete interacting with the surface of the organoid, lying perpendicular to the surface. Scale bar 100 µm.

(B right panel) Orthogonal view from 54 µm within the organoid. White box shows invaded spirochete in Z, X, and Y axis.

(C) Z-projections of BBB-organoids (magnification ×20) 24 h post-exposure to *B. garinii* LU116 showing the aggregation on the surface of each organoid. Each panel (A-D) shows a representative organoid from each group. $n^{\text{total organoids}} = 276$.

20 µm within the organoid (Figure 1B right panel and C). Distinct, individual spirochetes were also visualized at depths of 82–101 µm within BBB-organoids (Figure 1D). Quantification of single *Borrelia* spirochetes was confounded due to aggregation (Figure 1C); therefore, we quantified invasion as sub-surface volume (μm^3) of CFSE signal (Figure 2A). All five LNB associated *B. garinii* isolates had large volumes of CFSE signal below the surface of the BBB-organoids, whilst two of the *B. afzelii* isolates (LU68 and LU207) recorded some CFSE within the BBB-organoids (Figure 2A). They also showed evidence of diffuse, green-stained cells indicative of phagocytosis (Figure 2B).

B. burgdorferi induce volumetric changes and alterations in organoid integrity postexposure

In LNB swelling of the meninges leads to meningitis.[32] Recently, we demonstrated BBB-organoids to model the effect of the brain swelling observed in cerebral malaria, where parasites associated with cerebral malaria selectively altered the volume of organoids.[22] Here we used a similar approach to determine the impact of *Borrelia* spirochetes on BBB-organoids, and we measured the volume, morphology (round), and integrity (circularity) of each organoid 24 h post-exposure (Figures 3A–3C). Although there was a clear distinction between the LNB and non-LNB isolates with their ability to enter the organoids, all isolates induced an increase in volume except for a single isolate (*B. afzelii* LU81) which showed a decrease post-exposure (Figures 3A–3C). Further morphometric analysis of the organoids demonstrated they retained their general morphology (round), while their cohesion (circularity) and structural integrity was impaired (Figure 3D). Circularity measurements drastically decreased compared to controls for all but one isolate (*B. garinii* LU190 luc). To determine if this was a specific response to the *Borrelia* bacteria, or generalized toward any pathogen, we analyzed the gross morphology of organoids exposed to erythrocytes infected by *P. falciparum* isolates associated with cerebral malaria (Figure 3D). We have previously shown these isolates to selectively disrupt the BBB and induce swelling.[22] With *P. falciparum*-infected

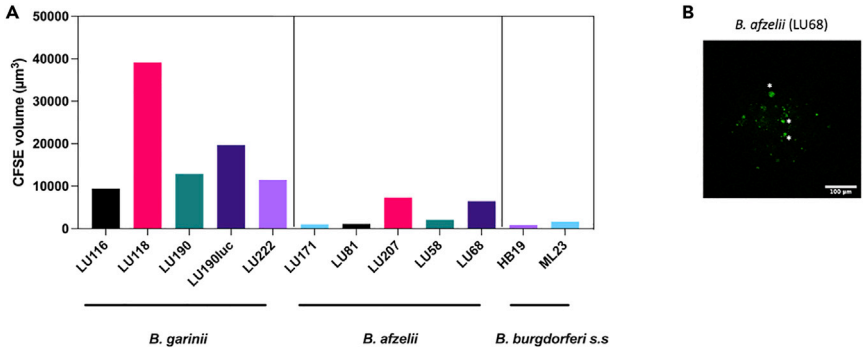

Figure 2. Volumetric quantification of sub-surface *Borrelia burgdorferi* within blood-brain barrier-organoids

(A) Graph plotting the total volume (µm^3) of carboxyfluorescein succinimidyl ester (CFSE) signal within the organoids after 24 h exposure to *B. garinii*, *B. afzelii*, and *B. burgdorferi* s. s.

(B) Maximum intensity Z-projection of CFSE signal from *B. afzelii* LU68 exposed organoid (magnification ×20). White asterisk denotes diffuse green stain indicative of phagocytosis. Scale bar 100 µm. $n^{\text{total organoids}} = 276$.

erythrocytes, we observed no alterations in the gross morphology of the organoids, and the roundness and circularity values were comparable to untreated controls, underpinning the observation that the negative responses by the organoids are specific to *Borrelia* exposure (Figure 3D). The *B. burgdorferi* s.l. exposed BBB-organoids presented with multiple fragmented nuclei and giant cells extending and detaching from the outer surface. The cellular cytoskeleton visualized with phalloidin showed multiple foci and irregular staining compared to the untreated control BBB-organoids (Figures 4A–4C).

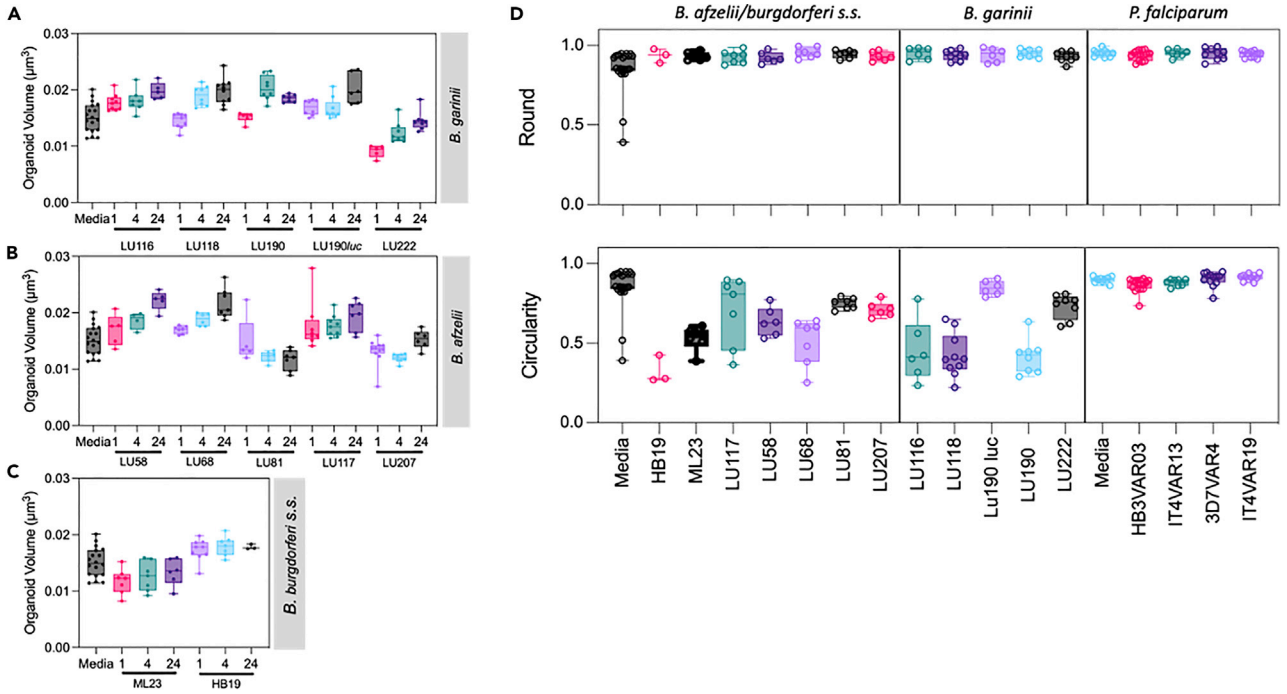

Figure 3. Morphometric analysis of blood-brain barrier-organoids post-exposure with *Borrelia burgdorferi*

The BBB organoids were co-incubated with ten different isolates of *B. burgdorferi* s. l., and two isolates of *B. burgdorferi* s. s. (Table 1), and red blood cells infected (IRBC) by four different *P. falciparum* lines.

Box and whisker plots, showing min/max values (A–D) of BBB-organoid volume (µm^3). Graphs (A–C) showed alterations post-*Borrelia* exposure. The gross morphology of organoids was measured by organoid roundness, i.e., general shape (D top panel), or the circularity i.e., organoid integrity. (D bottom panel). BBB-organoids were also exposed to *P. falciparum* lines (D both panels). The *P. falciparum* lines associated with cerebral (HB3VAR03, PFD1235w) has been shown to cross the BBB of organoids, while malaria parasites associated with uncomplicated (IT4VAR13, IT4VAR19) malaria did not.[22] $n^{\text{total organoids}} = 276$ (*Borrelia*), $n^{\text{total organoids}} = 61$ (*P. falciparum*).

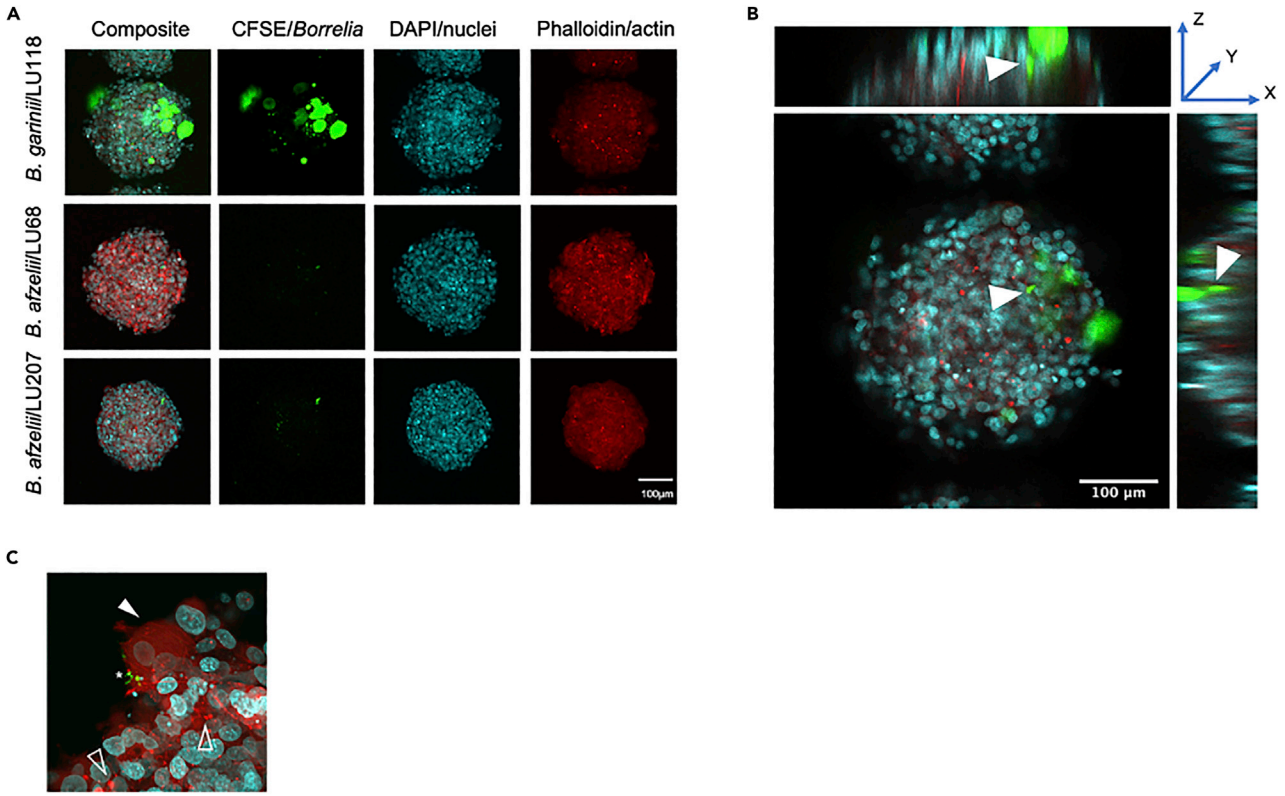

Figure 4. Internalization of *Borrelia* by blood-brain barrier-organoids

Blood-brain barrier (BBB)-organoids co-incubated with *B. burgdorferi* s. l. isolates.

(A) 3D Z-projection of organoids (magnification ×20) showing Carboxyfluorescein succinimidyl ester (CFSE stained) *Borrelia* in green, nuclei in blue (DAPI), and actin in red (phalloidin). The organoids were exposed to neurotropic (*B. garinii* LU118) or non-neurotrophic (*B. afzelii* LU207 and LU68) spirochetes. Composite images show overlays of CSFE, DAPI, and phalloidin stained images.

(B) Orthogonal view of organoid exposed to *B. garinii* LU118.White filled arrows point toward a large aggregate of spirochetes extending from the surface and into the organoid.

(C) Z-projection of BBB-organoid (magnification ×63) showing giant cell (white arrow) extending from the surface. Open arrows point to actin foci (phalloidin, red), whilst the asterisk denotes *B. garinii* LU116 spirochetes extending from surface into the cell (CFSE, green). Scale bar 100 µm. $n^{\text{total spheroids}}$ = 276 total.

B. burgdorferi spirochetes result in loss of tight junctions but fail to trigger significant cell death in organoids

The gross morphological analysis of the organoids exposed to spirochetes demonstrated a loss of integrity (Figures 3A–3C). To determine if exposure was impacting the expression of tight-junctions, organoids were co-incubated for 24 h with spirochetes representing each of the groups tested (ML23, LU118, and LU68). After fixation, organoids were stained for the tight-junction protein ZO-1 and imaged with a confocal microscope. Mock treated controls showed intact tight junctions, with staining localized around the periphery of cells and within the cytosol (Figure 5A top panel). Organoids treated with VEGF (50 ng/mL) a known disruptor of tight junctions show diffuse staining in the cytosol and not at the periphery (Figure 5B middle panel). Line intensity plots show peak fluorescence intensity at the peripheral boundary of the organoid, with no fluorescence in the center (Figure 5, bottom panel). Organoids exposed to ML23, LU118, or LU68 spirochetes display a fluorescence pattern similar to VEGF treated organoids, where fluorescence intensity is low and diffuse, demonstrating that the junctions have been disrupted (Figures 5C–5E). Given the observed loss of integrity and tight junctions (Figures 3D and 5C-5E), a live/dead assay was performed to assess the degree of cell death among the organoids exposed to the different *Borrelia* spp. Organoids were exposed to ML23, LU118, or LU68 spirochetes for 24 h, then imaged with a confocal microscope. Live cells stain intensely green, and interestingly, spirochete exposed organoids showed little evidence of cell death (red stain) and were comparable to the mock treated organoids (Figures 6A–6D). In contrast, the negative control organoids that were treated with 70% ethanol (EtOH) for 20 min before staining show mostly dead cells (red,

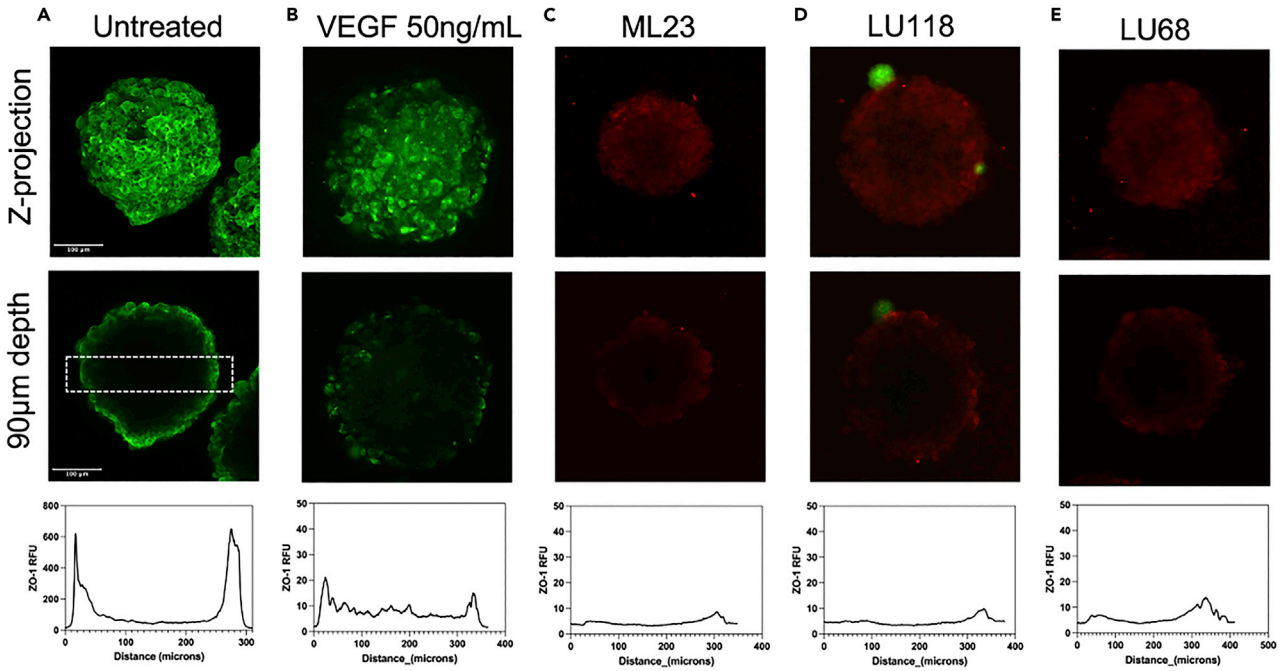

Figure 5. Spirochete exposure leads to a loss of tight junctions

Representative confocal images of organoids exposed to spirochetes for 24 h were fixed and then stained for the tight junction protein ZO-1 (green, AF488). (A) Z-projection of mock treated organoids showing bright ZO-1 stain around the periphery of the cells and diffuse within the cytosol. The dashed line from slices imaged at 90 μm depth (middle panel) represents the position analyzed to generate the intensity plots of ZO-1 stain (bottom panel).

(B) Organoids exposed to vascular endothelial growth factor (VEGF), show disrupted tight junctions and diffuse stain, while those exposed to (C) *B. burgdorferi* s.s. ML23, (D) *B. garinii* LU118, or (E) *B. afzelii* LU68 show low intensity, diffuse stain (red, AF647) $n^{\text{total spheroids}} = 60$ total. Scale bar = 100 μm.

Figure 6E). Analysis of the fold change in fluorescence intensity confirms very little cell death between the mock treated controls or *Borrelia*-exposed organoids; while the EtOH treated organoids had an almost 4-fold increase in fluorescence intensity (Figure 6F).

DISCUSSION

BBB-organoids provide a unique opportunity to investigate the neurotropic properties of different pathogens. They are comprised of the same component cells found *in vivo* and can self-assemble within 48 h.[29] Although they present with an "inside-out" cellular architecture compared to that found *in vivo*, they readily form tight junctions, control the passage of solutes, and with the endothelial cells exposed on the outer surface, making them ideal for investigating the effect pathogens have on the BBB.[22] Previous studies combining BBB-organoids and *P. falciparum* infected red blood cells show malaria parasites are taken up by brain endothelial cells, causing breakdown of the BBB, and swelling of BBB-organoids.[22,30] In this study, we show that *Borrelia* spirochetes readily enter the BBB-organoids and induce considerable alterations in both volume and integrity, and trigger loss of tight junctions. Of the panel of 12 isolates studied, all the *B. garinii* (5/5) genospecies readily colonized the BBB-organoid surface and invaded to depths of 20 μm. Single, intact spirochetes were observed even deeper at depths of 101 μm. In contrast, only two out of five *B. afzelii* entered the BBB-organoids. Indeed, there are reports of patients infected with *B. afzelii* presenting with LNB. There were several diffuse green cells observed within the BBB-organoids, indicating phagocytosis may have occurred. Exposure to any genospecies failed to trigger cell death in the organoids and though the integrity is significantly decreased, the cells within the organoids remain viable. Although endothelial cells, astrocytes, and pericytes important components of the BBB are not professional phagocytic cells, they are capable of clearing blood clots post-stroke and pathogens such as *P. falciparum* from their surface and extravasating them peri-vascularly.[22,33] The remaining *B. burgdorferi* s.s. isolates, including the tick isolate, failed to interact with the surface or enter the BBB-organoids. This variability in infectivity suggests that different genospecies have a varied affinity for the ability to cross the BBB and this may reflect the differences observed in clinical presentation of LB between different geographical locations.[34]

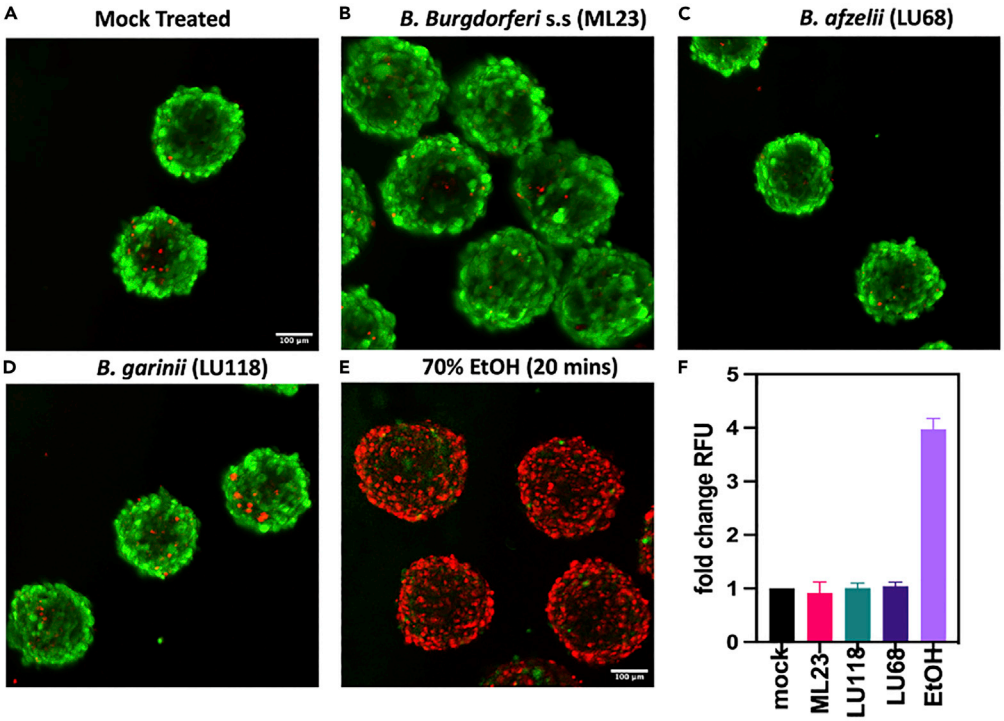

Figure 6. Live/Dead analysis of organoids post-spirochete exposure

(A–D) To determine the level of cell death post-spirochete exposure, organoids were treated with Live/Dead stain. Live cells in the organoids stain green, while dead cells stain red. Very few red stained are observed in the mock treated controls (A), or in the organoids exposed to (B) *B. burgdorferi* s.s. (B) ML23, (C) *B. garinii* LU118, or (D) *B. afzelii* LU68 spirochetes after 24 h co-incubation. The negative control organoids (E) were treated with 70% EtOH for 20 min and most cells were dead.

(F) plot showing the fold change in cell death compared to mock treated controls (+/−SD), with very little change post-spirochete exposure. $n^{\text{total spheroids}} = 60$ total. Scale bar = 100 μm.

The murine model has shown spirochetal entry into the meninges and induction of swelling.[14] Here, the majority of investigations examining the interactions between borrelial proteins and host tissues have concentrated upon other regions of the body and using cell lines such as human umbilical vein (HUVEC) and human brain microvascular cells (HBMEC), or cell lines derived from non-human sources.[35–38]

While there was a clear difference in the ability to enter the BBB-organoids, all spirochetes irrespective of genotype triggered alteration in the gross morphology and integrity of the BBB-organoids. This is in stark contrast to organoids exposed to red blood cells infected with *P. falciparum* isolates associated with cerebral malaria, the most frequently fatal form of malaria. On exposure to *P. falciparum*-infected red blood cells BBB-organoids demonstrated BBB-dysfunction (increased permeability), but not a lack of cell integrity.[22,39] Alterations in the actin cytoskeleton and nuclei are markers of cellular stress and inflammation and has been observed previously using endothelial monolayer experiments showing damage to cultured endothelial cells (HUVEC and HBMEC) after spirochete exposure.[38,40,41] Monolayer studies also identified the upregulation and triggering of plasminogen and metalloproteases post-exposure to *B. burgdorferi* s.l. spirochetes, and the initiation of the fibrinolytic cascade may contribute to BBB-dysfunction.[42,43]

The exact mechanism for crossing the BBB is not fully understood, and both paracellular and transcellular entry have been proposed.[42,44] Monolayer studies have identified a potential role for cell adhesion molecules such as E-selectin, ICAM-1, and VCAM-1, while other groups have implicated integrins and glycosaminoglycans such as heparan sulfate as playing a role.[45–47] Others have proposed that in place of a direct receptor-ligand interaction, *spirochetes* trigger cytokine release by host cells such as endothelial cells or neutrophils. These molecules trigger the opening of tight junctions, leading to paracellular migration across the endothelial layer. In the murine model, the role of neutrophils has been shown, and mice devoid of neutrophils have limited extravasation when infected with *borreliae*.[44] Our current model

demonstrates the migration of *B. garinii* isolates in the absence of immune cells. Tan et al. used derivates from *B. burgdorferi* strain B31, a tick isolate from North America where LNB is a rarely diagnosed. The ability to migrate in the absence of immune cells might contribute to the differences between the North American and European clinical presentations of LB. To our knowledge, this is the first study using organoids and a large panel of low passage *Borrelia* isolates from different biological origin and clinical manifestations in humans for studying *Borrelia* spp. and their impact on the BBB. Using low passage isolates avoids the risk of plasmid loss and genomic alternations due to prolonged *in vitro* culturing. Previous literature demonstrated the ability of *Borrelia* spp. to invade endothelial cells from HUVEC and HBMEC *in vitro*,[35,38] whereas murine infection studies also show organotropism, but use a limited number of isolates, or laboratory-adapted strains.[36,48,49] In conclusion, BBB-organoids appear to be an ideal model for LNB - not only for studies of the cellular and molecular biological mechanisms of spirochetal invasion of the CNS, but their ease of use, rapid generation, and reproducibility also make them suitable for screening chemotherapeutics for the treatment of LNB.

Limitations of the study

This study investigates at a limited number of *B. burgdorferi* s.l isolates LNB and future work could expand on this by assessing more isolates originating from different geographic and biological origin, and particularly *Borrelia* isolates confirmed to cause LB like *Borrelia bavariensis*, *Borrelia spielmanii*. and *Borrelia mayonii*, respectively. The BBB-organoids used for this study lack immune cells such as microglia, or other cells like oligodendrocytes which can contribute to the integrity of the BBB, and act as phagocytic cells in response to pathogens or damage.[50–53] While not the focus of this study, the model is expandable and to date a maximum of six different cell types have been cultured in tandem, including microglia and oligodendrocytes.[54,55] Taken together, these data highlight the usefulness of BBB-organoids for the investigation of neurotropic pathogens such as *B. burgdorferi* s.l.

STAR★METHODS

Detailed methods are provided in the online version of this paper and include the following:

- KEY RESOURCES TABLE
- RESOURCE AVAILABILITY
  - Lead contact
  - Materials availability
  - Data and code availability
- EXPERIMENTAL MODEL AND SUBJECT DETAILS
  - *B. burgdorferi* sensu lato and sensu stricto strains
  - Malaria parasites
  - Human cell cultures
- METHOD DETAILS
  - Blood-brain barrier-organoids
  - Co-culture of *Borrelia* spp. and 3D blood-brain barrier-organoids
  - Tight junction protein ZO-1 immunofluorescence and live/dead staining
- QUANTIFICATION AND STATISTICAL ANALYSIS
- ADDITIONAL RESOURCES

SUPPLEMENTAL INFORMATION

Supplemental information can be found online at https://doi.org/10.1016/j.isci.2022.105838.

ACKNOWLEDGMENTS

We thank Mette Ulla Madsen and the Core Facility for Integrated Microscopy, Faculty of Health and Medical Sciences, University of Copenhagen for excellent technical assistance. We also thank Professor Sven Bergström, Umeå University, Sweden, for kindly providing the clinical isolates of *B. burgdorferi* s.l. and Professor Jon Skare, Texas A&M University, USA for providing the plasmid pBBE22luc. The research performed at the Centre for Medical Parasitology, University of Copenhagen was supported by grants from the Danish Ministry of Food, Agriculture and Fisheries (3R-Center Research Grant), and the Lundbeck Foundation (R180-2014-3098, R313-2019-322 and R324-2019-2029). The research performed at the Department of Infectious Diseases, University Hospital, Rigshospitalet was supported by a grant from the Lundbeck

Foundation (R366-2021-127). This study was partially supported by a grant of the European Union through the European Regional DevelopmentFund and the Interreg NorthSea Region Program 2014–2020 as part of the NorthTick project (reference number J-No: 38-2-7-19).

AUTHOR CONTRIBUTIONS

A.R.J., Y.A., A.S.C., and A.M. L. were responsible for planning of experiments. A.R.J., Y.A., and A.M.L. were responsible for writing the manuscript A.R.J. and Y.A. were responsible for data interpretation and funding acquisition. A.R.J. was responsible for project strategy and management. Y.A. did the organoid production, performed experiments, and microscopy. P.W., A.H., M.L., P.E.L., P.K., A.K., and A.M.L. were responsible for the panel of *B. burgdorferi* ss./s.l. strains, A.S.C., M.L., K.N.K., and T.B. did the culturing. P.Ø.J. did the flow cytometry. All authors have critically reviewed the data and commented on the manuscript.

DECLARATION OF INTERESTS

Disclosures: Outside of the present work: A.M.L. reports speaker's honorarium/travel grants and advisory board activity from Gilead, GSK, and Pfizer. The other authors declare no competing interests exist. P.E.L. has been an external scientific expert to Valneva Austria GmbH and Pfizer Inc. and received speaker's honorarium and travel grants.

Received: June 13, 2022
Revised: November 16, 2022
Accepted: December 16, 2022
Published: January 20, 2023

REFERENCES

1. Kullberg, B.J., Vrijmoeth, H.D., van de Schoor, F., and Hovius, J.W. (2020). Lyme borreliosis: diagnosis and management. BMJ *369*, m1041. https://doi.org/10.1136/bmj.m1041.

2. Berglund, J., Eitrem, R., Ornstein, K., Lindberg, A., Ringér, A., Elmrud, H., Carlsson, M., Runehagen, A., Svanborg, C., and Norrby, R. (1995). An epidemiologic study of Lyme disease in southern Sweden. N. Engl. J. Med. *333*, 1319–1327. https://doi.org/10.1056/NEJM199511163332004.

3. Rupprecht, T.A., Koedel, U., Fingerle, V., and Pfister, H.-W. (2008). The pathogenesis of Lyme neuroborreliosis: from infection to inflammation. Mol. Med. *14*, 205–212. https://doi.org/10.2119/2007-00091.Rupprecht.

4. Garcia-Monco, J.C., and Benach, J.L. (2019). Lyme neuroborreliosis: clinical outcomes, controversy, pathogenesis, and polymicrobial infections. Ann. Neurol. *85*, 21–31. https://doi.org/10.1002/ana.25389.

5. Hansen, K., and Lebech, A.-M. (1992). The Clinical and Epidemiological profile of Lyme Neuroborreliosis in Denmark 1985-1990: a prospective study of 187 patients with Borrelia burgdorferi specific intrathecal antibody production. Brain *115*, 399–423. https://doi.org/10.1093/brain/115.2.399.

6. Hansen, K., Crone, C., and Kristoferitsch, W. (2013). Chapter 32 - Lyme neuroborreliosis. In Handbook of Clinical Neurology Peripheral Nerve Disorders, G. Said and C. Krarup, eds. (Elsevier), pp. 559–575. https://doi.org/10.1016/B978-0-444-52902-2.00032-1.

7. Kurokawa, C., Narasimhan, S., Vidyarthi, A., Booth, C.J., Mehta, S., Meister, L., Diktas, H., Strank, N., Lynn, G.E., DePonte, K., et al. (2020). Repeat tick exposure elicits distinct immune responses in Guinea pigs and mice. Ticks Tick Borne Dis. *11*, 101529. https://doi.org/10.1016/j.ttbdis.2020.101529.

8. Batool, M., Hillhouse, A.E., Ionov, Y., Kochan, K.J., Mohebbi, F., Stoica, G., Threadgill, D.W., Zelikovsky, A., Waghela, S.D., Wiener, D.J., and Rogovskyy, A.S. (2019). New Zealand white rabbits effectively clear Borrelia burgdorferi B31 despite the bacterium's functional vlsE antigenic variation system. Infect. Immun. *87*, e00164–e00219. https://doi.org/10.1128/IAI.00164-19.

9. Foley, D.M., Gayek, R.J., Skare, J.T., Wagar, E.A., Champion, C.I., Blanco, D.R., Lovett, M.A., and Miller, J.N. (1995). Rabbit model of Lyme borreliosis: erythema migrans, infection-derived immunity, and identification of Borrelia burgdorferi proteins associated with virulence and protective immunity. J. Clin. Invest. *96*, 965–975. https://doi.org/10.1172/JCI118144.

10. Appel, M.J., Allan, S., Jacobson, R.H., Lauderdale, T.L., Chang, Y.F., Shin, S.J., Thomford, J.W., Todhunter, R.J., and Summers, B.A. (1993). Experimental Lyme disease in dogs produces arthritis and persistent infection. J. Infect. Dis. *167*, 651–664. https://doi.org/10.1093/infdis/167.3.651.

11. Ornstein, K., Berglund, J., Nilsson, I., Norrby, R., and Bergström, S. (2001). Characterization of Lyme Borreliosis Isolates from Patients with Erythema Migrans and Neuroborreliosis in Southern Sweden. Journal of Clinical Microbiology *39*, 1294–1298. https://doi.org/10.1128/JCM.39.4.1294-1298.2001.

12. Steere, A.C., Grodzicki, R.L., Kornblatt, A.N., Craft, J.E., Barbour, A.G., Burgdorfer, W., Schmid, G.P., Johnson, E., and Malawista, S.E. (1983). The Spirochetal Etiology of Lyme Disease. New England Journal of Medicine *308*, 733–740. https://doi.org/10.1056/NEJM198303313081301.

13. Hyde, J.A. (2017). Borrelia burgdorferi Keeps Moving and Carries on: A Review of Borrelial Dissemination and Invasion. Frontiers in Immunology *8*.

14. Casselli, T., Divan, A., Vomhof-DeKrey, E.E., Tourand, Y., Pecoraro, H.L., and Brissette, C.A. (2021). A murine model of Lyme disease demonstrates that Borrelia burgdorferi colonizes the dura mater and induces inflammation in the central nervous system. PLoS Pathog. *17*, e1009256. https://doi.org/10.1371/journal.ppat.1009256.

15. Divan, A., Casselli, T., Narayanan, S.A., Mukherjee, S., Zawieja, D.C., Watt, J.A., Brissette, C.A., and Newell-Rogers, M.K. (2018). Borrelia burgdorferi adhere to blood vessels in the dura mater and are associated with increased meningeal T cells during murine disseminated borreliosis. PLoS One *13*, e0196893. https://doi.org/10.1371/journal.pone.0196893.

16. Gadila, S.K.G., Rosoklija, G., Dwork, A.J., Fallon, B.A., and Embers, M.E. (2021). Detecting Borrelia spirochetes: a case study with validation among autopsy specimens. Front. Neurol. *12*, 628045.

17. MacDonald, A.B. (1986). Borrelia in the brains of patients dying with dementia. JAMA *256*, 2195–2196.

18. MacDonald, A.B., and Miranda, J.M. (1987). Concurrent neocortical borreliosis and Alzheimer's disease. Hum. Pathol. *18*, 759–761. https://doi.org/10.1016/s0046-8177(87)80252-6.

19. Miklossy, J., Kasas, S., Zurn, A.D., McCall, S., Yu, S., and McGeer, P.L. (2008). Persisting atypical and cystic forms of Borrelia burgdorferiand local inflammation in Lyme neuroborreliosis. J. Neuroinflammation *5*, 40. https://doi.org/10.1186/1742-2094-5-40.

20. Dupin, N., Lecuyer, H., Carlotti, A., Poyart, C., Coureuil, M., Chanal, J., Schmitt, A., Vacher-Lavenu, M.-C., Taha, M.-K., Nassif, X., and Morand, P.C. (2012). Chronic meningococcemia cutaneous lesions involve meningococcal perivascular invasion through the remodeling of endothelial barriers. Clin. Infect. Dis. *54*, 1162–1165. https://doi.org/10.1093/cid/cis120.

21. Kolappan, S., Coureuil, M., Yu, X., Nassif, X., Egelman, E.H., and Craig, L. (2016). Structure of the Neisseria meningitidis Type IV pilus. Nat. Commun. *7*, 13015. https://doi.org/10.1038/ncomms13015.

22. Adams, Y., Olsen, R.W., Bengtsson, A., Dalgaard, N., Zdioruk, M., Satpathi, S., Behera, P.K., Sahu, P.K., Lawler, S.E., Qvortrup, K., et al. (2021). Plasmodium falciparum erythrocyte membrane protein 1 variants induce cell swelling and disrupt the blood–brain barrier in cerebral malaria. J. Exp. Med. *218*, e20201266. https://doi.org/10.1084/jem.20201266.

23. Disson, O., and Lecuit, M. (2012). Targeting of the central nervous system by Listeria monocytogenes. Virulence *3*, 213–221. https://doi.org/10.4161/viru.19586.

24. Hussain, B., Fang, C., and Chang, J. (2021). Blood–brain barrier breakdown: an emerging biomarker of cognitive impairment in normal aging and dementia. Front. Neurosci. *15*, 688090.

25. Al-Bachari, S., Naish, J.H., Parker, G.J.M., Emsley, H.C.A., and Parkes, L.M. (2020). Blood–brain barrier leakage is increased in Parkinson's disease. Front. Physiol. *11*, 593026.

26. Kamintsky, L., Cairns, K.A., Veksler, R., Bowen, C., Beyea, S.D., Friedman, A., and Calkin, C. (2020). Blood-brain barrier imaging as a potential biomarker for bipolar disorder progression. Neuroimage Clin. *26*, 102049. https://doi.org/10.1016/j.nicl.2019.102049.

27. Dudek, K.A., Dion-Albert, L., Lebel, M., LeClair, K., Labrecque, S., Tuck, E., Ferrer Perez, C., Golden, S.A., Tamminga, C., Turecki, G., et al. (2020). Molecular adaptations of the blood–brain barrier promote stress resilience vs. depression. Proc. Natl. Acad. Sci. USA *117*, 3326–3336. https://doi.org/10.1073/pnas.1914655117.

28. Dion-Albert, L., Cadoret, A., Doney, E., Kaufmann, F.N., Dudek, K.A., Daigle, B., Parise, L.F., Cathomas, F., Samba, N., Hudson, N., et al. (2022). Vascular and blood-brain barrier-related changes underlie stress responses and resilience in female mice and depression in human tissue. Nat. Commun. *13*, 164. https://doi.org/10.1038/s41467-021-27604-x.

29. Urich, E., Patsch, C., Aigner, S., Graf, M., Iacone, R., and Freskgård, P.O. (2013). Multicellular self-assembled spheroidal model of the blood brain barrier. Sci. Rep. *3*, 1500. https://doi.org/10.1038/srep01500.

30. Cho, C.-F., Wolfe, J.M., Fadzen, C.M., Calligaris, D., Hornburg, K., Chiocca, E.A., Agar, N.Y.R., Pentelute, B.L., and Lawler, S.E. (2017). Blood-brain-barrier spheroids as an in vitro screening platform for brain-penetrating agents. Nat. Commun. *8*, 15623. https://doi.org/10.1038/ncomms15623.

31. Adams, Y., and Jensen, A.R. (2022). 3D organoid assay of the impact of infected erythrocyte adhesion on the blood–brain barrier. In Malaria Immunology: Targeting the Surface of Infected Erythrocytes Methods in Molecular Biology, A.T.R. Jensen and L. Hviid, eds. (Springer US)), pp. 587–599. https://doi.org/10.1007/978-1-0716-2189-9_44.

32. Ramesh, G., Didier, P.J., England, J.D., Santana-Gould, L., Doyle-Meyers, L.A., Martin, D.S., Jacobs, M.B., and Philipp, M.T. (2015). Inflammation in the pathogenesis of Lyme neuroborreliosis. Am. J. Pathol. *185*, 1344–1360. https://doi.org/10.1016/j.ajpath.2015.01.024.

33. Lam, C.K., Yoo, T., Hiner, B., Liu, Z., and Grutzendler, J. (2010). Embolus extravasation is an alternative mechanism for cerebral microvascular recanalization. Nature *465*, 478–482. https://doi.org/10.1038/nature09001.

34. Andreasen, A.M., Dehlendorff, P.B., Knudtzen, F.C., Bødker, R., Kjær, L.J., and Skarphedinsson, S. (2020). Spatial and temporal patterns of Lyme neuroborreliosis on funen, Denmark from 1995–2014. Sci. Rep. *10*, 7796. https://doi.org/10.1038/s41598-020-64638-5.

35. Grab, D.J., Nyarko, E., Nikolskaia, O.V., Kim, Y.V., and Dumler, J.S. (2009). Human brain microvascular endothelial cell traversal by Borrelia burgdorferi requires calcium signaling. Clin. Microbiol. Infect. *15*, 422–426. https://doi.org/10.1111/j.1469-0691.2009.02869.x.

36. Caine, J.A., and Coburn, J. (2015). A short-term Borrelia burgdorferi infection model identifies tissue tropisms and bloodstream survival conferred by adhesion proteins. Infect. Immun. *83*, 3184–3194. https://doi.org/10.1128/IAI.00349-15.

37. Embers, M.E., Hasenkampf, N.R., Jacobs, M.B., Tardo, A.C., Doyle-Meyers, L.A., Philipp, M.T., and Hodzic, E. (2017). Variable manifestations, diverse seroreactivity and post-treatment persistence in non-human primates exposed to Borrelia burgdorferi by tick feeding. PLoS One *12*, e0189071. https://doi.org/10.1371/journal.pone.0189071.

38. Comstock, L.E., and Thomas, D.D. (1991). Characterization of Borrelia burgdorferi invasion of cultured endothelial cells. Microb. Pathog. *10*, 137–148. https://doi.org/10.1016/0882-4010(91)90074-K.

39. Lennartz, F., Adams, Y., Bengtsson, A., Olsen, R.W., Turner, L., Ndam, N.T., Ecklu-Mensah, G., Moussiliou, A., Ofori, M.F., Gamain, B., et al. (2017). Structure-guided identification of a family of dual receptor-binding PfEMP1 that is associated with cerebral malaria. Cell Host Microbe *21*, 403–414. https://doi.org/10.1016/j.chom.2017.02.009.

40. Gergel, E.I., and Furie, M.B. (2001). Activation of endothelium by Borrelia burgdorferi in vitro enhances transmigration of specific subsets of T lymphocytes. Infect. Immun. *69*, 2190–2197. https://doi.org/10.1128/IAI.69.4.2190-2197.2001.

41. Tkáčová, Z., Bhide, K., Mochnáčová, E., Petroušková, P., Hruškovicová, J., Kulkarni, A., and Bhide, M. (2021). Comprehensive mapping of the cell response to Borrelia bavariensis in the brain microvascular endothelial cells in vitro using RNA-seq. Front. Microbiol. *12*, 760627.

42. Grab, D.J., Perides, G., Dumler, J.S., Kim, K.J., Park, J., Kim, Y.V., Nikolskaia, O., Choi, K.S., Stins, M.F., and Kim, K.S. (2005). Borrelia burgdorferi, host-derived proteases, and the blood-brain barrier. Infect. Immun. *73*, 1014–1022. https://doi.org/10.1128/IAI.73.2.1014-1022.2005.

43. Gebbia, J.A., Monco, J.C., Degen, J.L., Bugge, T.H., and Benach, J.L. (1999). The plasminogen activation system enhances brain and heart invasion in murine relapsing fever borreliosis. J. Clin. Invest. *103*, 81–87. https://doi.org/10.1172/JCI5171.

44. Tan, X., Petri, B., DeVinney, R., Jenne, C.N., and Chaconas, G. (2021). The Lyme disease spirochete can hijack the host immune system for extravasation from the microvasculature. Mol. Microbiol. *116*, 498–515. https://doi.org/10.1111/mmi.14728.

45. Sellati, T.J., Abrescia, L.D., Radolf, J.D., and Furie, M.B. (1996). Outer surface lipoproteins of Borrelia burgdorferi activate vascular endothelium in vitro. Infect. Immun. *64*, 3180–3187. https://doi.org/10.1128/iai.64.8.3180-3187.1996.

46. Ebnet, K., Brown, K.D., Siebenlist, U.K., Simon, M.M., and Shaw, S. (1997). Borrelia burgdorferi activates nuclear factor-kappa B and is a potent inducer of chemokine and adhesion molecule gene expression in endothelial cells and fibroblasts. J. Immunol. *158*, 3285–3292.

47. Böggemeyer, E., Stehle, T., Schaible, U.E., Hahne, M., Vestweber, D., and Simon, M.M. (1994). Borrelia burgdorferi upregulates the adhesion molecules E-selectin, P-selectin, ICAM-1 and VCAM-1 on mouse endothelioma cells in vitro. Cell Adhes. Commun. *2*, 145–157. https://doi.org/10.3109/15419069409004433.

48. Lin, Y.-P., Tan, X., Caine, J.A., Castellanos, M., Chaconas, G., Coburn, J., and Leong, J.M. (2020). Strain-specific joint invasion and colonization by Lyme disease spirochetes is promoted by outer surface protein C. PLoS Pathog. *16*, e1008516. https://doi.org/10.1371/journal.ppat.1008516.

49. Coburn, J., Medrano, M., and Cugini, C. (2002). Borrelia burgdorferi and its tropisms for adhesion molecules in the joint. Curr. Opin. Rheumatol. *14*, 394–398. https://doi.org/10.1097/00002281-200207000-00010.

50. Hanisch, U.-K., and Kettenmann, H. (2007). Microglia: active sensor and versatile effector cells in the normal and pathologic brain. Nat. Neurosci. *10*, 1387–1394. https://doi.org/10.1038/nn1997.

51. Greenmyer, J.R., Gaultney, R.A., Brissette, C.A., and Watt, J.A. (2018). Primary human microglia are phagocytically active and respond to Borrelia burgdorferi with upregulation of chemokines and cytokines. Front. Microbiol. *9*, 811. https://doi.org/10.3389/fmicb.2018.00811.

52. Kimura, I., Dohgu, S., Takata, F., Matsumoto, J., Watanabe, T., Iwao, T., Yamauchi, A., and Kataoka, Y. (2020). Oligodendrocytes upregulate blood-brain barrier function through mechanisms other than the PDGF-BB/PDGFRα pathway in the barrier-tightening effect of oligodendrocyte progenitor cells. Neurosci. Lett. *715*, 134594.

53. Bradl, M., and Lassmann, H. (2010). Oligodendrocytes: biology and pathology. Acta Neuropathol. *119*, 37–53. https://doi.org/10.1007/s00401-009-0601-5.

54. Kumarasamy, M., and Sosnik, A. (2021). Heterocellular spheroids of the neurovascular blood-brain barrier as a platform for personalized nanoneuromedicine. iScience *24*, 102183. https://doi.org/10.1016/j.isci.2021.102183.

55. Sokolova, V., Mekky, G., van der Meer, S.B., Seeds, M.C., Atala, A.J., and Epple, M. (2020). Transport of ultrasmall gold nanoparticles (2 nm) across the blood–brain barrier in a six-cell brain spheroid model. Sci. Rep. *10*, 18033. https://doi.org/10.1038/s41598-020-75125-2.

56. Hubálek, Z., Halouzka, J., and Heroldová, M. (1998). Growth temperature ranges of Borrelia burgdorferi sensu lato strains. J. Med. Microbiol. *47*, 929–932. https://doi.org/10.1099/00222615-47-10-929.

57. Olsen, R.W., Ecklu-Mensah, G., Bengtsson, A., Ofori, M.F., Kusi, K.A., Koram, K.A., Hviid, L., Adams, Y., and Jensen, A.T.R. (2019). Acquisition of IgG to ICAM-1-binding DBLβ domains in the Plasmodium falciparum erythrocyte membrane protein 1 antigen family varies between Groups A, B and C. Infect. Immun. *87*, e00224–e00319. https://doi.org/10.1128/IAI.00224-19.

58. Bengtsson, A., Joergensen, L., Rask, T.S., Olsen, R.W., Andersen, M.A., Turner, L., Theander, T.G., Hviid, L., Higgins, M.K., Craig, A., et al. (2013). A novel domain cassette identifies Plasmodium falciparum PfEMP1 proteins binding ICAM-1 and is a target of cross-reactive, adhesion-inhibitory antibodies. J. Immunol. *190*, 240–249. https://doi.org/10.4049/jimmunol.1202578.

59. Lennartz, F., Bengtsson, A., Olsen, R.W., Joergensen, L., Brown, A., Remy, L., Man, P., Forest, E., Barfod, L.K., Adams, Y., et al. (2015). Mapping the binding site of a cross-reactive Plasmodium falciparum PfEMP1 monoclonal antibody inhibitory of ICAM-1 binding. J. Immunol. *195*, 3273–3283. https://doi.org/10.4049/jimmunol.1501404.

60. Joergensen, L., Bengtsson, D.C., Bengtsson, A., Ronander, E., Berger, S.S., Turner, L., Dalgaard, M.B., Cham, G.K.K., Victor, M.E., Lavstsen, T., et al. (2010). Surface Co-expression of two different PfEMP1 antigens on single Plasmodium falciparum-infected erythrocytes facilitates binding to ICAM1 and PECAM1. PLoS Pathog. *6*, e1001083. https://doi.org/10.1371/journal.ppat.1001083.

61. Skovsbo Clausen, A., Ørbæk, M., Renee Pedersen, R., Oestrup Jensen, P., Lebech, A.-M., and Kjaer, A. (2020). 64Cu-DOTATATE positron emission tomography (PET) of Borrelia burgdorferi infection: in vivo imaging of macrophages in experimental model of Lyme arthritis. Diagnostics *10*, 790. https://doi.org/10.3390/diagnostics10100790.

62. Schindelin, J., Arganda-Carreras, I., Frise, E., Kaynig, V., Longair, M., Pietzsch, T., Preibisch, S., Rueden, C., Saalfeld, S., Schmid, B., et al. (2012). Fiji: an open-source platform for biological-image analysis. Nat. Methods *9*, 676–682. https://doi.org/10.1038/nmeth.2019.

STAR★METHODS

KEY RESOURCES TABLE

REAGENT or RESOURCE	SOURCE	IDENTIFIER
Bacterial and virus strains		
HB19	Sven Bergström and Katharina Ornstein	N/A
ML23	Professor John Skare	N/A
LU58	Sven Bergström and Katharina Ornstein	N/A
LU68	Sven Bergström and Katharina Ornstein	N/A
LU171	Sven Bergström and Katharina Ornstein	N/A
LU207	Sven Bergström and Katharina Ornstein	N/A
LU116	Sven Bergström and Katharina Ornstein	N/A
LU118	Sven Bergström and Katharina Ornstein	N/A
LU190	Sven Bergström and Katharina Ornstein	N/A
LU190 luciferase	Professor Peter Kraiczy	N/A
LU222	Sven Bergström and Katharina Ornstein	N/A
Chemicals, peptides, and recombinant proteins		
Celltrace CFSE cell proliferation kit	Thermofisher	C34554
Phalloidin	Merck	P1951;RRID:AB_2315148
DAPI	Merck	D9542
Experimental models: Cell lines		
hCMEC/D3	Cederland Labs	CLU512;RRID:CVCL_U985
Astrocytes	Neuromics	HMP202
Pericytes	Neuromics	HMP104
Software and algorithms		
Fiji	open source	https://doi.org/10.1038/nmeth.2019
GraphPad Prism v9.5.0	GraphPad	https://www.graphpad.com/scientific-software/prism/

RESOURCE AVAILABILITY

Lead contact

Further information and requests may be directed to and will be fulfilled by the Lead Contact Yvonne Adams, yadams@sund.ku.dk (Y.A.).

Materials availability

This study did not generate new, unique reagents. The strains provided by Professor Sven Bergström were a kind gift for the purposes of the manuscript and ownership is retained by Professor Bergström.

Data and code availability

- All data is reported and available in this paper.
- This paper does not use or report original code.
- Any additional information required to reanalyze the data reported in this paper is available from the lead contact upon request.

EXPERIMENTAL MODEL AND SUBJECT DETAILS

B. burgdorferi sensu lato and sensu stricto strains

A panel of 12 *B. burgdorferi* s.l. patient isolates (Table 1) comprising different genotypes isolated from skin biopsies or cerebrospinal fluid was assessed. The genotypes included five *B. garinii* (LNB), five *B. afzelii* (LB),

and two *B. burgdorferi* s.s. (LB). The *Borrelia* spirochetes were cultured in Barbour-Stoenner-Kelly medium (BSK-H) supplemented with 6% rabbit serum (Merck KGaA, Darmstadt, Germany) under conventional microaerobic conditions (1–5% CO_2, 33°C) created in Oxoid™ Compact Plastic Pouches (Thermo Fisher Scientific, Waltham, MA) with a Oxoid™ Campygen™ Compact sachet (Thermo Fisher Scientific), sealed airtight with a sealing clip.[56] Growth was recorded using dark-field microscopy.

Malaria parasites

The *P. falciparum* lines selected for surface expression of specific *P. falciparum* erythrocyte membrane protein 1 (PfEMP1) molecules (*P. falciparum* 3D7 expressing PFD1235w, HB3 expressing HB3VAR03, and IT4 expressing IT4VAR13 or IT4VAR19) were maintained in *in vitro* blood culture and were selected using antibodies against DBLβ_D4 domains of specific PfEMP1s as previously described.[22,39,57,58] Phenotypes were verified by flow cytometry and Q-PCR as previously described.[39,57–60]

Human cell cultures

The human brain microvascular endothelial cell line (hCMEC)/D3 (CLU512, Cedarlane Labs, CA.) was maintained on collagen-coated (50 μg/mL, rat tail type I, BD Biosciences) flasks and grown in VascuLife VEGF – Mv media (LL0005, CellSystems) supplemented with rhVEGF (5 ng/mL), rhEGF (5 ng/mL), rhFGF (5 ng/mL), rhIGF-1 (15 ng/mL), L-Glutamine (10 mM), hydrocortisone hemisuccinate (1 μg/mL), heparin sulphate (0.75 U/mL), ascorbic acid (50 μg/mL), fetal bovine serum (FBS, 5%), 10,000 U/mL penicillin, 10,000 μg/mL streptomycin, and 25 μg/mL amphotericin B. Primary human brain microvascular pericytes and astrocytes (Neuromics, USA), were maintained on poly-L-lysine (10 μg/mL) coated flasks with pericyte (HMP104) and astrocyte (PGB003) growth medium (Neuromics). Astrocytes and pericytes were used at passages 3–5 and hCMEC/D3 at passage 27–29.

METHOD DETAILS

Blood-brain barrier-organoids

Human pericytes, primary astrocytes, and hCMEC/D3 released by 0.025% trypsin/EDTA (Sigma Aldrich, Saint Louis, MO) were resuspended in BBB-working medium (Vasculife-Mv supplemented with 2% normal human serum with antibiotics omitted), and 1.5 ×10^3 of each cell type (final volume of 100 μL/well) were seeded onto sterile 1% w/v solid agarose (Sigma) pre-dispensed into low binding 96-well plates (Thermo Fisher Scientific). A further 100 μL of BBB working media (BBBM) was added to bring the volume in each well to a total of 200 μL. Multicellular BBB organoids were allowed to self-assemble (48–72 h) in a humidified 5% CO_2-incubator at 37°C.[22,30] The orientation of the component cells was determined by pre-staining astrocytes with 1μM CellTrace Far Red (Thermo Fisher Scientific) for 20minat 37°C in the dark prior to assembling organoids. Staining for CD31 on endothelial cells and NG2 on pericytes was performed post-formation. Once organoids formed, they were washed, pooled, and fixed with 3.7% formaldehyde for 10 min prior to staining for 45 min with anti-CD31 (1:200, R&D Systems) and anti-NG2 (1:200, Millipore) post-permeabilization with 0.1% Triton X-100. The receptors were visualized with anti-mouse-IgG Alexa Fluor 450 (CD31) and anti-rabbit-IgG Alexa Flour 488 (NG2). Images were captured with Zeiss LSM 780 and line plot analysis conducted in Fiji.

Co-culture of *Borrelia* spp. and 3D blood-brain barrier-organoids

Borrelia isolates were grown in 5 mL BSK-H medium for 7 days prior to assay. On day 7, spirochetes were stained with 5 μM Syto 9 (Thermo Fisher Scientific) and with 5 μM Syto 60 (Thermo Fisher Scientific) before determination of the cell density using flow cytometry.[61] The bacteria were washed three times in phosphate-buffered saline (PBS), centrifuged 3minat 5500 × g, and resuspended in CFSE (Invitrogen) in PBS (500 μL) was added to a final concentration of 5 μM CFSE and incubated 10 min in the dark at room temperature. Spirochetes were washed twice with PBS containing 5% FBS adjusted to 30,000 *B. burgdorferi* s.l./well in BBBM and BSK-H medium (1:1 ratio). Spirochetes were added (100 μL/well) and incubated at 37°C for 1, 4, and 24 h. At the end of the assay, organoids were pooled in groups, then washed in PBS and fixed for 10 min in 3.7% v/v formaldehyde. The organoids were transferred to 12-well chamber slides (Ibidi, Germany), following incubation with Phalloidin and DAPI (300 nM), prior to being imaged with a Zeiss LSM 780 confocal microscope (Zeiss, Germany). Z-stacks were captured to 102.8 μm depth at 2.32 μm intervals (×10). To determine the amount of *B. burgdorferi* s.l. sp. within each organoid, the color channels were split in Fiji, and the 3D objects counter was deployed to calculate the volume of CFSE signal (green channel) throughout the Z-stack. The volume was calculated for each

organoid and expressed as total CFSE volume (μm^3) per organoid. The volume of individual organoids (mm^3), circularity, and roundness were calculated from (×20) brightfield images at 102.8 μm depth from diameter measurements generated in Fiji.[62] To calculate volume, the following equation was used, $V = 4/3\pi r^3$. To calculate circularity the following equation was used 4π*area/perimeter^2, while roundness is calculated using the following formula - 4*area/(π*major axis)^2.

Tight junction protein ZO-1 immunofluorescence and live/dead staining

Organoids were exposed to *Borrelia* spp. for 24 h, then pooled in groups and washed in PBS before fixing for 10 min in 3.7% v/v formaldehyde. Organoids were permeabilized with 0.1% Triton X-100 for 5 min, before washing (PBS + 5% goat serum) prior to staining with anti-ZO-1 (Thermo Fisher) 1:200 for 45 min. The organoids were then washed (PBS+5% goat serum) before incubating for 45 min in the dark with anti-goat Alexa Fluor 488, or Alexa Fluor 647 at room temperature. Organoids were washed, incubated with DAPI (300 nM), then transferred to 12-well chamber slides (Ibidi, Germany) prior to being imaged a Zeiss LSM 780 confocal microscope (Zeiss, Germany). Z-stacks were captured to 102.8 μm depth at 2.32 μm intervals (×10). The amount of cell death post-spirochete exposure was determined using Live/Dead stain (Thermo Fisher). The positive control group were pre-treated for 20 min with 70% EtOH prior to staining to kill the organoids. Images were captured using Zeiss LSM780 confocal microscope. Line plot analysis was performed on the resulting images using Fiji.

QUANTIFICATION AND STATISTICAL ANALYSIS

Confocal images were analyzed using Fiji and results plotted with GraphPad Prism 9. Specific information for each experiment can be found in the figure legends.

ADDITIONAL RESOURCES

This paper did not create any additional resources.